AIAA JOURNAL
Vol. 33, No. 2, February 1995

Multilevel Decomposition Procedure for Efficient Design Optimization of Helicopter Rotor Blades

Aditi Chattopadhyay,* Thomas R. McCarthy,† and Narayanan Pagaldipti†
Arizona State University, Tempe, Arizona 85287

This paper addresses a multilevel decomposition procedure, for efficient design optimization of helicopter blades, with the coupling of aerodynamics, blade dynamics, aeroelasticity, and structures. The multidisciplinary optimization problem is decomposed into three levels. The rotor is optimized for improved aerodynamic performance at the first level. At the second level, the objective is to improve the dynamic and aeroelastic characteristics of the rotor. A structural optimization is performed at the third level. Interdisciplinary coupling is established through the use of optimal sensitivity derivatives. The Kreisselmeier–Steinhauser function approach is used to formulate the optimization problem when multiple design objectives are involved. A nonlinear programming technique and an approximate analysis procedure are used for optimization. Results obtained show significant improvements in the rotor aerodynamic, dynamic, and structural characteristics, when compared with a reference or baseline rotor.

Nomenclature

AI	= autorotational inertia, lb-ft^2
C_P	= power coefficient
C_T	= thrust coefficient
c	= chord, ft
c_0–c_3	= chord distribution parameters, ft
EI_{xx}	= lagging stiffness, lb-ft^2
EI_{zz}	= flapping stiffness, lb-ft^2
F_k	= objective functions
F_{k_0}	= values of F_k at the beginning of an iteration
f	= K-S function constraint vector
f_r	= 3/rev radial shear, lb
f_x	= 3/rev in-plane shear, lb
f_z	= 4/rev vertical shear, lb
g	= constraint functions
K	= total number of constraints and objective functions
m_c	= 3/rev torsional moment, lb-ft
m_x	= 3/rev flapping moment, lb-ft
m_z	= 4/rev lagging moment, lb-ft
R	= blade radius, ft
T	= thrust, lb
W	= total blade weight, lb
w_{0j}	= nonstructural weight at jth node, lb
x, y, z	= reference axes
$\bar{y}$	= nondimensional radial location
α_j	= real part of the jth stability root
ε_k	= kth objective function tolerance
θ	= blade twist, deg
θ_1–θ_3	= blade twist parameters, deg
μ	= advance ratio
ρ	= K-S function multiplier
σ	= area-weighted solidity
σ_r	= blade root centrifugal stress, lb/ft^2
υ_j	= minimum allowable damping of jth stability root
ϕ	= design variable vector
Ω	= rotor angular velocity, rpm

Received Feb. 3, 1994; revision received Sept. 21, 1994; accepted for publication Sept. 30, 1994.

*Associate Professor, Department of Mechanical and Aerospace Engineering. Senior Member AIAA.

†Graduate Research Assistant, Department of Mechanical and Aerospace Engineering. Student Member AIAA.

Introduction

In recent years, optimization techniques have received wide attention in helicopter rotor blade design for addressing various design issues involving dynamics, aerodynamics, structures, and aeroelasticity. Considerable research on aeroelastic optimization of metal rotor blades has been performed during the last decade as indicated by Friedmann.[1] Chattopadhyay and Walsh[2] addressed vibration reduction and minimum weight design of rotor blades with stress constraints. Recently, Ganguli and Chopra[3] developed an aeroelastic optimization and sensitivity analysis procedure for composite hingeless rotors using an analytical approach. Most of these research efforts were based on a single discipline.

Rotary wing aircraft design is truly multidisciplinary in nature, and therefore an integration of the necessary disciplines is essential for an optimization procedure to be meaningful. Celi and Friedmann[4] addressed the coupling of dynamic and aeroelastic criteria, using quasisteady airloads, for blades with straight and swept tips. An integrated aerodynamic and dynamic optimization procedure was presented by Chattopadhyay et al.[5] The integration of aerodynamic loads and dynamics was achieved by coupling the necessary comprehensive analysis procedures inside a closed-loop optimization technique. He and Peters[6] performed a combined structural, dynamic, and aerodynamic optimization of rotor blades using a simple box beam model to represent the structural component in the blade. Chattopadhyay and McCarthy[7,8] developed multicriteria optimization procedures for the design of helicopter rotor blades. The objectives were to reduce blade vibration with the coupling of blade dynamics, aerodynamics, aeroelasticity and structures. Very recently, multidisciplinary optimization efforts have also been initiated to investigate the design of high-speed proprotors by Chattopadhyay and Narayan[9] and Chattopadhyay et al.[10]

Since the validity of the designs obtained using optimization techniques depends strongly upon the accuracy of the analysis procedures used, it is essential to integrate sufficiently comprehensive analysis tools within the closed-loop optimization procedure. Such procedures are computationally intensive and, hence, can be prohibitive within an optimization environment. Furthermore, the problem becomes highly coupled and is accompanied by a large number of design variables. Therefore, an "all-at-once" optimization procedure in which all of the disciplines are coupled inside a single loop and optimization is performed based on criteria involving every discipline can be inefficient and time consuming. Therefore, decomposition techniques are often used to simplify such complex optimization problems into a number of subproblems. Multilevel decomposition techniques have been applied to problems based on a single discipline[11–15] in structural applications. In a multidisciplinary design problem, the number of levels in a multilevel

decomposition procedure depends upon the number of disciplines involved. Individual optimization is performed at each level using analysis procedures pertaining to that level. Optimal sensitivity parameters are exchanged between the levels to provide the necessary coupling between the levels. An optimal design is obtained when each individual level is converged and overall convergence is achieved. Therefore, the speed of obtaining a fully converged result depends upon the strength of coupling between the various levels. Adelman et al.[16] developed a two-level procedure for performing integrated aerodynamic, dynamic, and structural optimization of rotor blades, based on the multilevel optimization strategy described in Ref. 14. In the upper level, the blade was optimized for a combination of aerodynamic and dynamic performance with constraints on the aerodynamic, dynamic, and structural behavior. In the lower level, the internal blade structure was designed to provide sufficient stiffnesses and section masses needed at the upper level. However, several important dynamic design criteria were not included in the formulation. Also, aeroelastic stability, which is an important criterion in forward flight, was not considered. Finally, a linear combination was used to combine the multiple objective functions. This procedure is judgmental because weight factors are used to combine the individual objective functions, which does not guarantee improvements of the individual objective functions in accordance with the weights imposed on them. In this paper, a three-level procedure is developed to further address the complex helicopter rotor blade design problem and to introduce additional disciplinary couplings. Design criteria pertaining to aerodynamics, dynamics, aeroelastic stability, and structures are included. Interdisciplinary constraints are imposed on the individual optimizations performed at each level. A multiobjective optimization technique, which is effective in combining several objective functions and constraints into a composite envelope function, is used where necessary.

Multilevel Decomposition

The multidisciplinary design problem is formulated using a three-level decomposition procedure illustrated here. Each level is a multiobjective optimization problem characterized by a vector of objective functions, constraints, and design variables. The formulation is outlined next, where NOBJ = number of objective functions, NC = number of constraints, and NDV = number of design variables.

Level 1

Minimize

$$F_i^1(\phi_1) \qquad i = 1, \ldots, \text{NOBJ}^1$$

subject to

$$g_k^1(\phi_1) \le 0 \qquad k = 1, \ldots, \text{NC}^1$$

$$\sum_{i=1}^{\text{NDV}^1} \frac{\partial F_j^{2*}}{\partial \phi_i^1} \Delta\phi_i^1 \le \varepsilon_{2j} \qquad j = 1, \ldots, \text{NOBJ}^2$$

$$\sum_{i=1}^{\text{NDV}^1} \frac{\partial F_j^{3*}}{\partial \phi_i^1} \Delta\phi_i^1 \le \varepsilon_{3j} \qquad j = 1, \ldots, \text{NOBJ}^3$$

$$\phi_i^{1L} \le \phi_i^1 \le \phi_i^{1U} \qquad i = 1, \ldots, \text{NDV}^1$$

$$\phi_j^{2L} \le \phi_j^{2*} + \sum_{i=1}^{\text{NDV}^1} \frac{\partial \phi_j^{2*}}{\partial \phi_i^1} \Delta\phi_i^1 \le \phi_j^{2U} \qquad j = 1, \ldots, \text{NDV}^2$$

$$\phi_j^{3L} \le \phi_j^{3*} + \sum_{i=1}^{\text{NDV}^1} \frac{\partial \phi_j^{3*}}{\partial \phi_i^1} \Delta\phi_i^1 \le \phi_j^{3U} \qquad j = 1, \ldots, \text{NDV}^3$$

where F^1, F^2, and F^3 are the objective function vectors at levels 1, 2, and 3, respectively; g^1, g^2, and g^3 are the corresponding constraint vectors; and ϕ^1, ϕ^2, and ϕ^3 are the corresponding design variable vectors. The quantities ε_j^2 and ε_j^3 represent tolerances on the changes in the jth objective functions corresponding to levels 2 and 3, respectively. Superscripts L and U refer to lower and upper bounds, respectively, and superscript * represents optimum values. The quantities $\partial F_j^{2*}/\partial \phi_i^1$ and $\partial F_j^{3*}/\partial \phi_i^1$ are the optimal sensitivity derivatives of the objective functions used at levels 2 and 3, respectively, with respect to the design variables at level 1. Finally, $\partial \phi_j^{2*}/\partial \phi_i^1$ and $\partial \phi_j^{3*}/\partial \phi_i^1$ are the optimal sensitivity derivatives of the design variables vectors at levels 2 and 3, respectively, with respect to the design variables at level 1. The optimal sensitivity derivatives can be calculated using the technique described in Ref. 17.

Level 2

Minimize

$$F_j^2(\phi^{1*}, \phi^2) \qquad j = 1, \ldots, \text{NOBJ}^2$$

subject to

$$g_k^2(\phi^{1*}, \phi^2) \le 0 \qquad k = 1, \ldots, \text{NC}^2$$

$$\sum_{i=1}^{\text{NDV}^2} \frac{\partial F_j^{3*}}{\partial \phi_i^2} \Delta\phi_i^2 \le \varepsilon_{3j} \qquad j = 1, \ldots, \text{NOBJ}^3$$

$$\phi_i^{2L} \le \phi_i^2 \le \phi_i^{2U} \qquad i = 1, \ldots, \text{NDV}^2$$

$$\phi_j^{3L} \le \phi_j^{3*} + \sum_{i=1}^{\text{NDV}^2} \frac{\partial \phi_j^{3*}}{\partial \phi_i^2} \Delta\phi_i^2 \le \phi_j^{3U} \qquad j = 1, \ldots, \text{NDV}^3$$

where ϕ^{1*} is the optimum design variable vector from level 1. This vector is kept fixed during optimization at level 2. The optimal sensitivity derivatives of the level 3 objective functions and design variables with respect to level 2 design variables are denoted $\partial F_j^{3*}/\partial \phi_i^2$ and $\partial \phi_j^{3*}/\partial \phi_i^2$, respectively.

Level 3

Minimize

$$F_j^3(\phi^{1*}, \phi^{2*}, \phi^3) \qquad j = 1, \ldots, \text{NOBJ}^3$$

subject to

$$g_k^3(\phi^{1*}, \phi^{2*}, \phi^3) \le 0 \qquad k = 1, \ldots, \text{NC}^3$$

$$\phi_j^{3L} \le \phi_j^3 \le \phi_j^{3U} \qquad j = 1, \ldots, \text{NDV}^3$$

where the optimum vectors from upper levels, ϕ^{1*} and ϕ^{2*}, are held constant. The optimization procedure cycles through all three levels before global convergence is achieved. A "cycle" is defined as one complete sweep through all three levels of optimization. Optimization at an individual level also requires several "iterations" before local convergence is achieved. Cycling between the three levels is necessary to account for the coupling between the objective functions, constraints, and design variables pertaining to the various levels.

Problem Formulation

The decomposition of the helicopter rotor blade optimization problem is described here. A smart decomposition can decouple the problem efficiently and help achieve faster convergence. This can be accomplished through a knowledge of the design process and synthesis as well as the magnitudes of the optimal sensitivity derivatives. In the conventional design process of an aircraft, the planform variables are prescribed by the aerodynamicist. The desired stiffnesses of the wing are prescribed by the dynamicist and the structural engineer designs the wing structure with sufficient stiffnesses. Based on the previous concept, coupled with a knowledge of the optimal sensitivity parameters, the rotor design problem is decomposed into three levels.

Level 1

The rotor is optimized for improved aerodynamic performance at level 1 of the procedure. The total power coefficient C_P is the objective function. Level 1 design variables include spanwise variations of chord and twist distributions. A constraint is imposed on the rotor thrust coefficient C_T to insure the same lifting capability of the reference rotor. In order not to deviate too much from the baseline flight condition and also to ensure efficiency in hover a lower bound is imposed on the rotor solidity σ. The constraints are formulated as follows:

$$C_T = C_{T\text{ref}}$$

$$\sigma \geq \sigma_{\min}$$

where the subscript "ref" stands for the reference, or baseline, rotor, and the subscript "min" refers to the minimum allowable blade solidity. As required by the multilevel decomposition procedure, constraints are also imposed on the changes in the optimum values of second and third level objective functions and design variables. In this paper, the 4/rev vertical shear and the 3/rev in-plane shear, which are the second level objective functions as described in the next section, are constrained to be within 20% of their optimum values. The total blade weight, which is the third level objective function as described later, is constrained to be within 25% of its optimum value.

Level 2

At level 2, the objective is to improve the dynamic and aeroelastic characteristics of the rotor and control the vibratory and static stresses on the blade. For a four-bladed rotor in forward flight, the most critical vibratory hub loads occur at the fundamental blade passing frequency of 4/rev. This also includes contributions from the 3/rev and 5/rev loads as well.[18] However, the magnitudes of the 5/rev loads are small compared with the 3/rev loads and are therefore ignored. The six critical vibratory loads are the 4/rev vertical shear f_z, the 4/rev lagging moment m_z, the 3/rev in-plane shear f_x, the 3/rev radial shear f_r, the 3/rev flapping moment m_x, and 3/rev torsional moment m_c. In this problem, the 4/rev vertical shear f_z and the 3/rev in-plane shear f_x are included as objective functions since their values were found to be more significant. A constraint is imposed on the 3/rev radial force f_r. The moments are not included directly as constraints, but their magnitudes are checked during each design iteration. A lower bound is imposed on the autorotational inertia AI to insure that the rotor has sufficient inertia to autorotate in the event of engine failure. Constraints are also imposed on the real part of the stability roots to maintain aeroelastic stability. These constraints assume the following form:

$$f_r \leq f_{rU}$$

$$AI \geq AI_L$$

$$\alpha_k \leq -\upsilon, \qquad k = 1, 2, \ldots, K$$

where the subscripts U and L represent upper and lower bounds, respectively. The quantity α_k represents the real part of the stability root, K denotes the total number of modes, and υ denotes a minimum allowable blade damping, which is a positive number.

The design variables used in level 2 are discrete values of the flapping and lagging stiffnesses, EI_{zz_i} and EI_{xx_i}, respectively, at each segment ($i = 1, \ldots,$ NSEG and NSEG is the total number of blade segments). Discrete values of the nonstructural weights (Fig. 1) located at the blade tip, w_{0i}, ($i = 1, \ldots,$ NSEG) are also used as design variables. To reduce the amount of design variables at this level to reduce the computational effort, the values of the torsional rigidity GJ are estimated at this level based on changes in the flapping and lagging stiffnesses. The exact values for GJ are, however, calculated in the third level.

Level 3

At level 3, it is of interest to design the spar such that optimum structural stiffnesses from level 2 match the actual stiffnesses of the spar. The appropriate objective function is the total blade weight that is to be minimized. The five independent wall thicknesses (Fig. 1), at each section t_{j_i} ($j = 1, \ldots, 5$), are used as design variables.

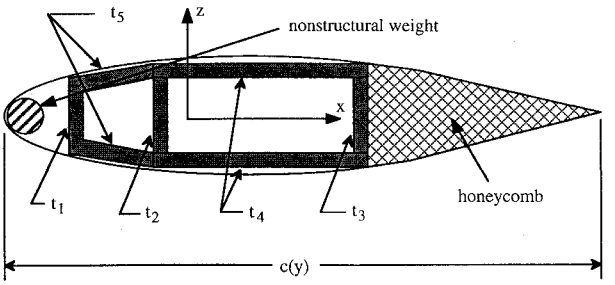

Fig. 1 Two-celled isotropic box beam.

To insure that the actual flapping and lagging stiffnesses are close to the optimum stiffnesses, as determined in level 2, these stiffnesses are constrained to be within a small tolerance of the optimum stiffnesses. An upper bound constraint $\sigma_{\max}$ is imposed on the blade centrifugal stress, at the root σ_r. The constraints are as follows:

$$|EI_{xx} - EI_{xx_{\text{opt}}}| \leq \varepsilon(EI_{xx_{\text{opt}}})$$

$$|EI_{zz} - EI_{zz_{\text{opt}}}| \leq \varepsilon(EI_{zz_{\text{opt}}})$$

$$\sigma_r \leq \sigma_{\max}/FS$$

where $EI_{xx_{\text{opt}}}$ and $EI_{zz_{\text{opt}}}$ are the optimum stiffnesses obtained from level 2, ε is the allowable tolerance on the deviations, FS is the factor of safety, and $\sigma_{\max}$ is the maximum allowable blade stress. It should be noted here that at this level all of the structural properties are calculated exactly based on the two-celled box beam. These exact values that are determined based on thin wall theory are then used to update all of the structural properties required.

Aerodynamic Model

The rotor blade aerodynamic model is described in this section. The blade chord and twist distributions are modeled as nonlinear functions of the nondimensionalized radius $\bar{y}$. The chord $c(\bar{y})$ and twist distributions $\theta(\bar{y})$ are defined to have the following spanwise variations:

$$c(\bar{y}) = c_0 + c_1(\bar{y} - 0.75) + c_2(\bar{y} - 0.75)^2 + c_3(\bar{y} - 0.75)^3 \quad (1)$$

$$\theta(\bar{y}) = \theta_1(\bar{y} - 0.75) + \theta_2(\bar{y} - 0.75)^2 + \theta_3(\bar{y} - 0.75)^3 \quad (2)$$

These distributions are chosen to closely model the properties of an existing blade.[19] The nonlinear distributions also allow the optimizer sufficient flexibility in the design space, since these parameters are used as design variables.

Structural Model

The load-carrying structural member in the rotor is modeled as a two-cell isotropic box beam (Fig. 1) with five independent wall thicknesses that are assumed to vary spanwise. Spanwise nonstructural tuning masses are located at 2.5% chord location. The beam is symmetrical about the x axis and is assumed to be the principal load-carrying member in the rotor. Outer dimensions of the box beam at a blade section are based on constant percentages of the chord at that particular section. Titanium is used as the blade material. Exact structural analyses are performed only in levels 1 and 3 since discrete values of the flapping and lagging stiffnesses are used as design variables at level 2.

Since the flapping and lagging stiffnesses are used as design variables in level 2, the remaining structural properties are estimated based on these values. For example, the polar moment of inertia I_θ, the torsional rigidity GJ, the shear center-center of gravity offset x_i, and the blade mass m are estimated based upon the current values of the flapping and lagging stiffnesses and the values of the respective stiffnesses from the last real analysis. All other physical blade properties are assumed to remain constant. From these values it is

then possible to estimate the total blade weight W, the autorotational inertia AI, and the centrifugal stress at the root σ_r.

Multiobjective Function Formulation

Because the optimization problem in level 2 involves more than one design objective, the Kreisselmeier–Steinhauser (K-S) function approach[20] is used. The first step in formulating the objective function in this approach involves transformation of the original objective functions into reduced objective functions.[8] These reduced objective functions assume the following form:

$$F_k^*(\Phi) = \frac{F_k(\Phi)}{F_{k_0}} - 1.0 - g_{\max} \leq 0 \qquad k = 1, \ldots, \text{NOBJ} \quad (3)$$

The quantity $g_{\max}$ is the value of the largest constraint corresponding to the design variable vector Φ and is held constant during each iteration. A new constraint vector $f_m(\Phi)$ ($m = 1, 2, \ldots, M$ where $M = \text{NC} + \text{NOBJ}$) is introduced that includes the original constraints and the constraints introduced by the reduced objective functions [Eq. (3)]. The design variable vector remains unchanged. The new objective function to be minimized is then defined using the K-S function as follows:

$$F_{\text{KS}}(\Phi) = f_{\max} + \frac{1}{\rho} \log_e \sum_{m=1}^{M} e^{\rho[f_m(\Phi) - f_{\max}]} \quad (4)$$

where $f_{\max}$ is the largest constraint corresponding to the new constraint vector $f_m(\Phi)$ and in general is not equal to $g_{\max}$. The optimization problem is thus reduced to an unconstrained minimization of the K-S function. Further details of this approach are found in Refs. 8 and 20.

Analysis and Optimization

The program CAMRAD[21] is used for the blade dynamic, aerodynamic, and aeroelastic stability analyses. The code uses lifting line theory, with corrections for yawed flow, to calculate the section loading based on the two-dimensional aerodynamic characteristics of the airfoil. At each cycle of the optimization procedure the blade is trimmed within CAMRAD so that the intermediate designs that are feasible designs represent trimmed configurations. A wind-tunnel trim option is used since the reference rotor represents an existing wind-tunnel model rotor. The rotor lift and drag, each normalized with respect to solidity and the flapping angle, are trimmed using the collective pitch, the cyclic pitch, and the shaft angle. An uniform inflow model is used in the analysis to reduce computational effort.

The optimized rotor is trimmed to the same value of the thrust coefficient C_T as the reference rotor using a variable trim procedure.[8] The blade response is calculated, in CAMRAD, using rotating free-vibration modes equivalent to a Galerkin analysis. Ten bending modes that include seven flap-dominated modes and three lead-lag dominated modes and three torsion modes are calculated. Main blade responses of up to 8/rev are included. Therefore, eight harmonics of the rotor revolution are retained in the airloads calculations. The vibratory shear forces and moments are calculated based upon the airloads information obtained from the aerodynamic analysis. The aeroelastic stability analysis is performed using Floquet theory for periodic state equations. Four bending degrees of freedom and one torsional degree of freedom are used for the stability analysis.

The blade section properties are based on thin wall theory and the structural analysis of the rotor blade is performed using an in-house code.[22] The code models a simple two-cell homogeneous box beam with one rectangular cell and one trapezoidal cell (Fig. 1). It is assumed that the flatwise, chordwise, and torsional stiffnesses of the blade are provided solely by the box beam.

The optimization algorithm, as implemented in the code CONMIN,[23] is a nonlinear programming technique based upon the method of feasible directions. A two-point exponential approximation technique[24] is used within the optimizer since exact evaluation of the objective functions and constraints during each iteration is computationally prohibitive. This technique is superior to the linear Taylor series approximation since it contains gradient information from the current and previous cycles.

Results

The optimization procedure is applied to a reference blade of radius $R = 4.685$ ft and rotational velocity $\Omega = 639.5$ rpm that is operating in forward flight with an advance ratio $\mu = 0.3$. The rotor is an existing advanced four-bladed articulated rotor that represents a wind-tunnel model of the Growth Black Hawk rotor.[5] The blade is discretized into 10 segments (NSEG = 10). A summary of the operating conditions is presented in Table 1. The physical constraints imposed during optimization include the blade solidity σ, the autorotational inertia AI, the centrifugal stress at the blade root σ_r, the minimum allowable blade damping υ, and the 3/rev in-plane vibratory shear force f_r. A value of $\sigma_{\min} = 0.100$ is used as the lower bound on the solidity, and the upper bound used on the autorotational inertia is 19.8 lb-ft^2. A minimum allowable blade damping of $\upsilon = 0.01$ is used for all modes to ensure that the optimum blade retains damping. The reference value of $f_r = 1.11$ lb is used as the upper bound on the 3/rev in-plane shear force. The root centrifugal stress is constrained to be below 12.5×10^6 lb/ft^2, which is calculated using the allowable stress for titanium and a factor of safety $FS = 2$. These values are based on the reference rotor.

A total of seven aerodynamic design variables are used in level 1 to define the chord and twist distributions. In level 2, 30 design variables are used to define the discrete spanwise variations of the flapping and lagging stiffnesses and the nonstructural weights. In level 3, the 5 individual wall thicknesses of the two-celled isotropic box beam lead to a total of 50 design variables along the span. Therefore, the entire multilevel decomposition optimization procedure consists of a total of 87 design variables. Global convergence is achieved in only 3 cycles, each cycle requiring 5 iterations in level 1, 15 iterations in level 2, and 4 iterations in level 3.

The optimum results are presented in Tables 2 and 3 and Figs. 2–8. It is seen from Table 2 and Fig. 2 that there are significant reductions in the individual objective functions from all levels. The objective function in level 1, the coefficient of total power C_P, is reduced by 19.8%. The 4/rev vertical shear f_z, one of the objective functions in level 2, is reduced by 45.8%. The second objective function in level 2, the 3/rev in-plane shear f_x, remains equal to the reference value. The large reduction in f_z and no reduction in f_x are possibly because the K-S function envelope follows the f_z surface more closely than f_x due to the value of the K-S factor ρ selected for this problem. It must also be noted that the procedure does not guaran-

Table 1 Summary of operating conditions

Blade radius R, ft	4.685
Rotor thrust T, lb	277
Rotational velocity Ω, rpm	639.5
Advance ratio μ	0.3

Table 2 Summary of optimum results

	Bounds			
	Lower	Upper	Reference	Optimum
Objective functions				
Level 1				
C_P			0.000470	0.000377
Level 2				
f_z, lb			0.204	0.111
f_x, lb			1.41	1.41
Level 3				
W, lb			5.95	5.73
Constraints				
Level 1				
σ	0.100	——	0.116	0.104
Level 2				
f_r	——	1.11	1.11	1.00
AI, lb-ft^2	19.8	——	39.4	33.9
Level 3				
σ_r, $\times 10^6$ lb/ft^2	——	12.5	1.51	1.51
Trim, C_T/σ			0.0592	0.0659

Table 3 Box beam wall thicknesses

	Box beam wall thicknesses, in.									
NSEG	1	2	3	4	5	6	7	8	9	10
Reference	0.0625	0.0625	0.0625	0.0625	0.0625	0.0625	0.0625	0.0625	0.0625	0.0625
t_1	0.0612	0.0613	0.0621	0.0601	0.0621	0.0648	0.0633	0.0631	0.0617	0.0636
t_2	0.0570	0.0495	0.0611	0.0431	0.0699	0.1105	0.0668	0.0670	0.0530	0.0453
t_3	0.0602	0.0551	0.0631	0.0469	0.0658	0.0820	0.0642	0.0657	0.0583	0.0636
t_4	0.0423	0.0585	0.0530	0.0825	0.0511	0.0693	0.0940	0.0766	0.0568	0.0749
t_5	0.0488	0.0422	0.0608	0.0290	0.0728	0.1032	0.0783	0.0711	0.0444	0.0225

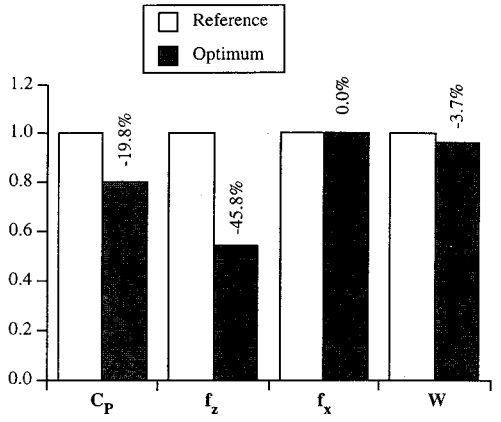

Fig. 2 Summary of optimum results.

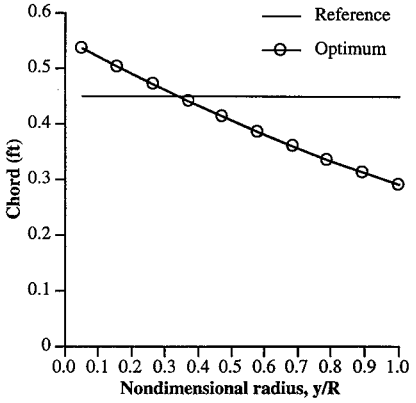

Fig. 3 Blade chord distributions.

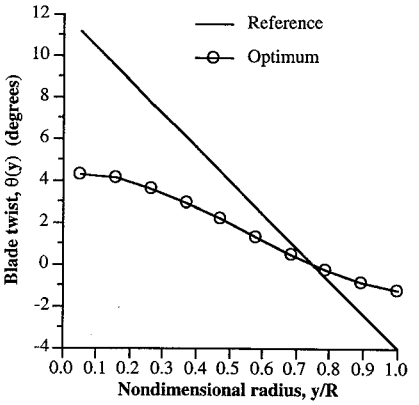

Fig. 4 Blade twist distributions.

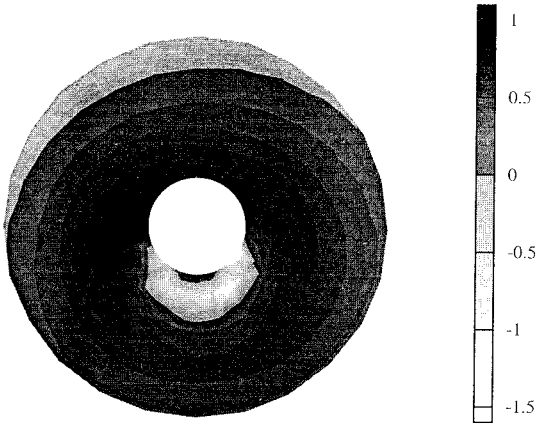

Fig. 5a Lift coefficient distributions for reference rotors.

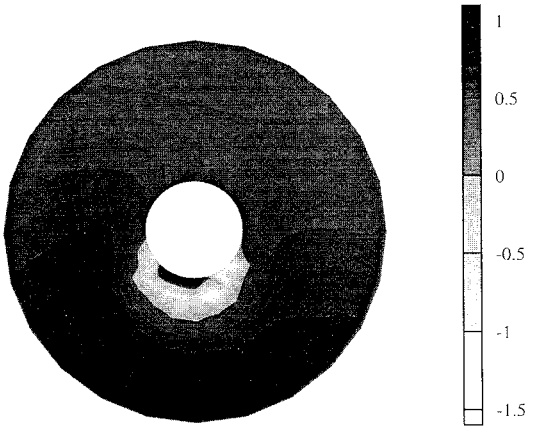

Fig. 5b Lift coefficient distributions for optimum rotors.

tee a global optimum; therefore the solution obtained represents a local minimum. The total blade weight W, which is the objective function in level 3, is reduced by 3.7%. As summarized in Table 2, the constraints for all three levels are well satisfied. The constraints imposed upon the autorotational inertia and the centrifugal stress are always well satisfied, whereas the solidity becomes nearly active for the optimum blade. The 3/rev radial shear force is reduced by 9.5% during the optimization procedure.

The chord and twist distributions, which are defined by level 1 design variables, are presented in Figs. 3 and 4. From Fig. 3 it is seen that optimum blade has a nearly linear tapered planform, despite the fact that the assumed chord distribution is cubic. As a consequence, the blade solidity is reduced from reference to optimum blade. This also implies that the optimum rotor is operating at a slightly higher C_T/σ value while maintaining the same rotor thrust as the reference rotor (Table 2). The optimum configuration being tapered represents a more aerodynamically efficient design with a more evenly distributed load distribution. The twist distribution is shown in Fig. 4 where significant changes are observed. The reference rotor has a linear twist distribution with nearly 16 deg of total twist, from root to tip. The optimum rotor has a highly nonlinear distribution, and the total twist is significantly reduced (approximately 6 deg, from

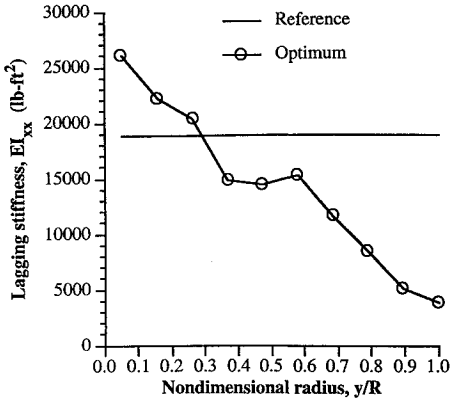

Fig. 6 Lagging stiffness distributions.

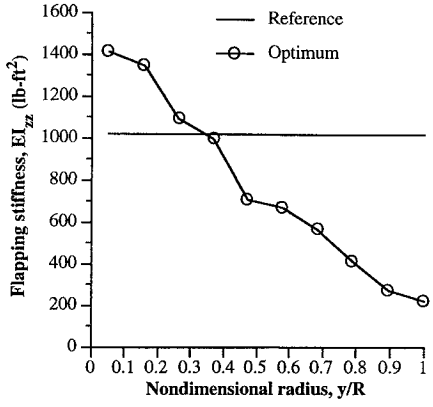

Fig. 7 Flapping stiffness distributions.

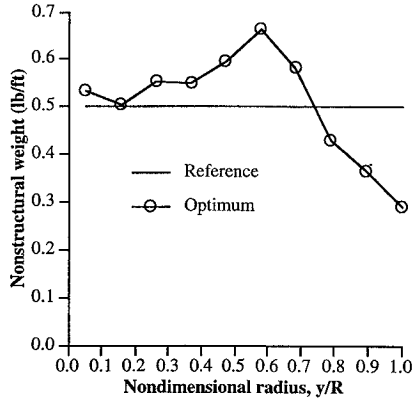

Fig. 8 Nonstructural weight distributions.

root to tip). As seen in Figs. 5a and 5b, the overall reduction in the blade twist has the effect of reducing the region of negative angles of attack in the optimum rotor map compared with the reference rotor, thereby improving aerodynamic efficiency. It is of interest to note that the advancing blade encounters negative angles at the tip in the reference rotor (Fig. 5a). The performance is significantly improved by optimization, and this region of negative angles of attack is completely alleviated in the optimum rotor (Fig. 5b).

The level 2 design variables are shown in Figs. 6–8. Both the lagging stiffness EI_{xx} and the flapping stiffness EI_{zz} have similar trends. Because of the optimal sensitivity derivatives, there is a very strong dependence of the stiffnesses on the chord distribution determined in level 1. This is because as the chord changes, the dimensions of the box beam also change. Figure 6 shows the lagging stiffness distribution where the similarities between the stiffness and chord distributions are observed. Similar trends are also observed in the flapping stiffness distribution (Fig. 7). The nonstructural weight w_0 distributions are presented in Fig. 8. When compared with the reference rotor, there is an increase in the magnitudes of

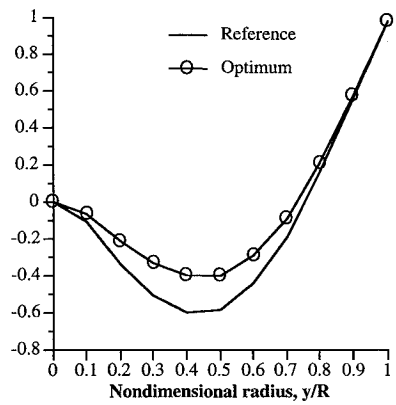

Fig. 9 First elastic flap dominated mode.

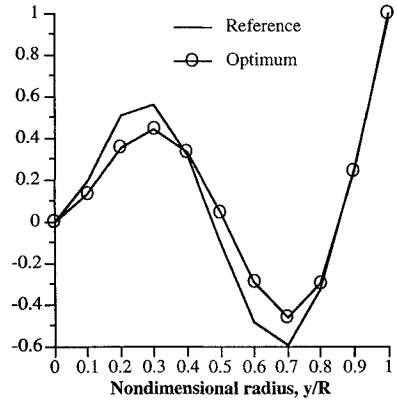

Fig. 10 Second elastic flap dominated mode.

these weights from root to 75% span followed by a subsequent decrease. This trend represents a compromise between the optimizer's effort in altering the dynamic response while reducing the blade weight. The nonlinearities in the stiffnesses and nonstructural weight distributions are due to the optimizer's effort in altering the mode shapes (make them more orthogonal to the forcing function) to reduce vibration. The elastic mode shapes of the optimum and reference rotors for the first two flap and lead-lag dominated and the first torsion mode are shown in Figs. 9–13. The general trend in each of these distributions is to reduce the amplitude of the modes at the inboard and midspan locations of the blade. This has the effect of reducing the vibration over a significant portion of the blade, which reduces the overall vibration at the root. The trend is particularly evident in the first elastic torsion mode (Fig. 13). It must be noted that the principal nature of the modes remains unaltered during optimization. Although the autorotational inertia is used as a constraint, this constraint is always well satisfied and therefore does not influence the nonstructural weight distribution significantly.

The design variables of level 3 are presented in Table 3, which shows the discrete spanwise variations of all five independent box beam wall thicknesses of the reference and optimum blades. The nonlinearities in the distributions are a result of the objective in level 3, which is to obtain a minimum weight structure that satisfies the stiffness distributions as predicted by level 2. Such a beam would be very impractical to build using isotropic materials, but the stiffness distributions can be easily achieved through composite tailoring.

Figure 14 shows the real and imaginary parts of the characteristic exponents, which are level 2 constraints, for the optimum and reference rotors. It is seen that aeroelastic stability is maintained after optimization and that the blade has higher damping than the minimum prescribed value ($\upsilon = 0.01$).

In summary, the multilevel procedure developed is efficient in formulating and addressing multidisciplinary design optimization of rotary wing aircraft. The decomposition helps in understanding the coupling between the various disciplinary criteria and the design variable linkage. The design objectives and constraints are

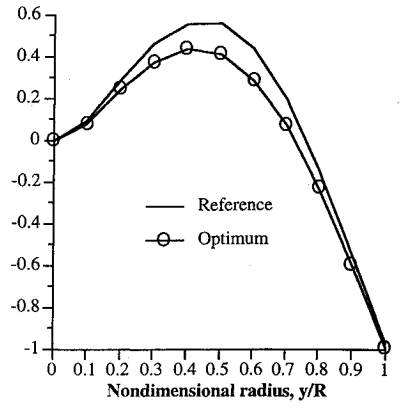

Fig. 11 First elastic lead-lag dominated mode.

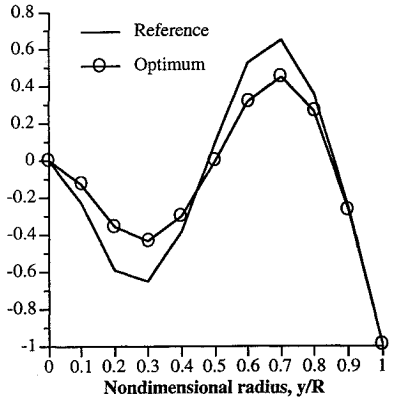

Fig. 12 Second elastic lead-lag dominated mode.

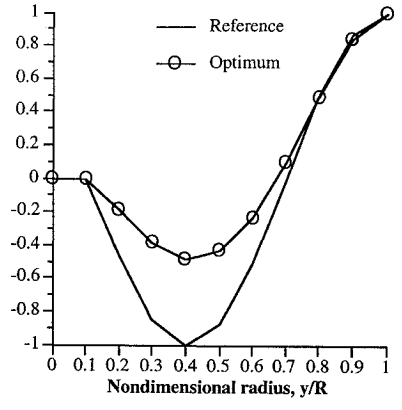

Fig. 13 First elastic torsion mode.

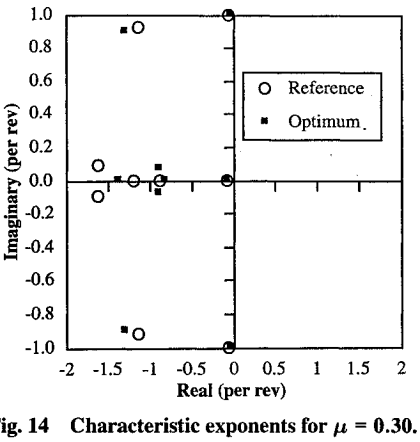

Fig. 14 Characteristic exponents for $\mu = 0.30$.

all satisfied in the example shown. The results obtained must be viewed within the context of the modeling assumptions used in the analysis. However, the procedure provides realistic design trends in rotary blade design and important tradeoffs associated with the coupling of aerodynamics, dynamics, aeroelastic stability, and structures.

Concluding Remarks

A multilevel, multidisciplinary decomposition procedure has been developed for the optimal design of helicopter rotor blades. Blade aerodynamic, dynamic, aeroelastic, and structural design requirements have been coupled within a three-level decomposition optimization procedure. In level 1, the coefficient of total power is reduced using aerodynamic design variables. Level 2 comprises two objectives functions to be reduced, the 4/rev vertical shear and the 3/rev in-plane shear. The two objective function problem is formulated using the Kreisselmeier–Steinhauser function approach. The design variables used are discrete spanwise distributions of the flapping and lagging stiffnesses and nonstructural weights. At level 3, the objective is to obtain a minimum weight spar design to satisfy the stiffnesses predicted by level 2. The design variables are discrete spanwise distributions of the five independent box beam wall thicknesses. A nonlinear programming approach is used in conjunction with a hybrid approximation technique. The procedure yields significant design improvements. The following specific observations are made within the context of the modeling assumptions used.

1) The multilevel decomposition optimization procedure yielded significant reductions in the objective functions in all three levels. The use of the decomposition technique allowed for more identifiable interpretations of the results, and its inclusion within the optimization procedure made the overall optimization problem more efficient.

2) The optimization procedure yielded a more efficient rotor with improved lift distributions.

3) The coefficient of total power was significantly reduced due to the more optimal chord and twist distributions obtained in level 1.

4) Blade vibration was improved significantly through stiffness and mass tailoring. The mode shapes were also altered in an effort to reduce vibration. The flapping and lagging stiffness distributions followed the chord distribution due to the use of optimal sensitivity derivatives, which linked the two levels.

5) The optimum rotor configuration remained aeroelastically stable throughout the optimization procedure even though stiffness and mass distributions were significantly altered.

6) The procedure yielded a significantly lighter rotor with improved overall performance.

Acknowledgments

This research was supported by NASA Ames Research Center under Grant NAG 2-771, with technical monitors John F. Madden III and Sesi Kottapalli, and Grant NCA 2-778, with technical monitor Thomas A. Edwards.

References

[1]Friedmann, P. P., "Helicopter Vibration Optimization Using Structural Optimization with Aeroelastic/Multidisciplinary Constraints," *Journal of Aircraft*, Vol. 28, No. 1, 1991, pp. 8–21.

[2]Chattopadhyay, A., and Walsh, J. L., "Minimum Weight Design of Rotorcraft Blades with Multiple Frequency and Stress Constraints," *AIAA Journal*, Vol. 28, No. 3, 1990, pp. 565–567.

[3]Ganguli, R., and Chopra, I., "Aeroelastic Optimization of a Helicopter Rotor with Composite Tailoring," American Helicopter Society 49th Annual Forum, St. Louis, MO, 1993.

[4]Celi, R., and Friedmann, P. P., "Efficient Structural Optimization of Rotor Blades with Straight and Swept Tips," *Proceedings of the 13th European Rotorcraft Forum* (Arles, France), 1987.

[5]Chattopadhyay, A., Walsh, J. L., and Riley, M. F., "Integrated Aerodynamic/Dynamic Optimization of Helicopter Blades," *Journal of Aircraft*, Vol. II, No. 1, 1991, pp. 58–65 (special issue on Multidisciplinary Optimization of Aeronautical Systems).

[6]He, C., and Peters, D. A., "Optimization of Rotor Blades for Combines Structural, Dynamic and Aerodynamic Properties," *Proceedings of the Third Airforce/NASA Symposium on Recent Advances in Multidisciplinary Analysis and Optimization* (San Francisco, CA), 1990.

[7]Chattopadhyay, A., and McCarthy, T. R., "Recent Efforts at Multicriteria Design Optimization of Helicopter Rotor Blades," NATO/DFG ASI, Berchtesgaden, Germany, Sept. 1991, see also *Stuctural Optimization* (submitted for publication).

[8]Chattopadhyay, A., and McCarthy, T. R., "Multidisciplinary Optimization of Helicopter Rotor Blades Including Design Variable Sensitivity," *Engineering Composites*, Vol. 3, No. 1, 1993.

[9]Chattopadhyay, A., and Narayan, J., "Optimum Design of High Speed Prop-Rotors Using a Multidisciplinary Approach," *Engineering Optimization*, Vol. 22, 1993, pp. 1–17.

[10]Chattopadhyay, A., McCarthy, T. R., and Madden, J. F., "An Optimization Procedure for the Design of Prop-Rotors in High Speed Cruise Including the Coupling of Performance, Aeroelastic Stability and Structures," *Mathematical and Computer Modelling*, Vol. 19, No. 3/4, 1994, pp. 75–88 (special issue on Rotorcraft).

[11]Schmit, L. A., and Merhinfar, M., "Multilevel Optimum Design of Structures with Fiber-Composite Stiffened-Panel Components," *AIAA Journal*, Vol. 20, No. 1, 1982, pp. 138–147.

[12]Schmit, L. A., and Chang, K. J., "A Multilevel Method for Structural Synthesis," AIAA/ASME/AHS/ASCE 25th Structures, Structural Dynamics, and Materials Conference, Palm Springs, CA, 1984.

[13]Kirsch, U., "An Improved Multilevel Structural Synthesis Method," *Journal of Structural Mechanics*, Vol. 13, No. 2, 1985, pp. 123–144.

[14]Sobieszczanski-Sobieski, J., James, B. B., and Riley, M. F., "Structural Optimization by Generalized, Multilevel Optimization," AIAA/ASME/AHS/ASCE 26th Structures, Structural Dynamics, and Materials Conference, Orlando, FL, 1985.

[15]Barthelemy, J. F. M., and Riley, M. F., "Improved Multilevel Optimization Approach for the Design of Complex Engineering Systems," *AIAA Journal*, Vol. 26, No. 3, 1988, pp. 353–360.

[16]Adelman, H. M., Walsh, J. L., and Pritchard, J. I., "Recent Advances in Integrated Multidisciplinary Optimization of Rotorcraft," AIAA/USAF/NASA/OAI 4th Symposium on Multidisciplinary Analysis and Optimization, AIAA Paper 92-4777-CP, Cleveland, OH, 1992.

[17]Sobieszczanski-Sobieski, J., and Barthelemy, J. F. M., "Sensitivity of Optimum Solutions to Problem Parameters," *AIAA Journal*, Vol. 20, No. 9, 1982, pp. 1291–1299.

[18]Gessow, A., and Myers, G. C., *Aerodynamics of the Helicopter*, College Park Press, 1985.

[19]Chattopadhyay, A., and Chiu, Y. D., "An Enhanced Integrated Aerodynamic/Dynamic Approach to Optimum Rotor Blade Design," *Structural Optimization*, Vol. 4, 1992, pp. 75–84.

[20]Kreisselmeier, A., and Steinhauser, R., "Systematic Control Design by Optimizing a Vector Performance Index," *Proceedings of the IFAC Symposium on Computer Aided Design of Control Systems* (Zurich, Switzerland), 1979, pp. 113–117.

[21]Johnson, W., "A Comprehensive Analytical Model of Rotorcraft Aerodynamics and Dynamics," Pt. II, Users' Manual, NASA TM 81183, 1980.

[22]McCarthy, T. R., "An Integrated Multidisciplinary Optimization Approach for Rotary Wing Design," Master's Thesis, Arizona State Univ., Tempe, AZ, Dec. 1992.

[23]Vanderplaats, G. N., "CONMIN—A FORTRAN Program for Constrained Function Minimization," Users' Manual, NASA TMX 62282, 1973.

[24]Fadel, G. M., Riley, M. F., and Barthelemy, J. M., "Two Point Exponential Approximation Method for Structural Optimization," *Structural Optimization*, Vol. 2, pp. 117–224.